Supporting Information

Crystalline gas of 1,1,1-trichloroethane

Maciej Bujak[a], Marcin Podsiadło[b] and Andrzej Katrusiak[b]

[a]Faculty of Chemistry, University of Opole, Oleska 48, 45-052 Opole, Poland. E-mail: mbujak@uni.opole.pl; Fax: +48(77)452-7101; Tel:+48(77)452-7100; [b]Faculty of Chemistry, Adam Mickiewicz University, Grunwaldzka 6, 60-780 Poznań, Poland. E-mail: katran@amu.edu.pl; Fax: +48(61)829-1505; Tel: +48(61)829-1443

In-situ low-temperature and high-pressure crystal growth

The commercially available 1,1,1-trichloroethane, 111TCE, CH_3CCl_3 (Laboratory Reagent, Hopkin & Williams, England) was used without further purification. 111TCE was sealed in a glass capillary (the internal diameter of 0.3 mm and the wall 0.01 mm thick). The capillary was fixed on a standard goniometer head that was mounted on the goniometer of a diffractometer. The liquid sample, filling *ca.* 0.5 mm of the capillary, was cooled in a nitrogen gas stream from a Cryostream cooler (Oxford Cryosystems). The shock cooling, from the room temperature to 200 K, resulted in the formation of a sample containing a single crystal of acceptable quality for a data collection. To determine the structure close to the phase II → phase I transition temperature of 224 K, [R. Rudman and B. Post, *Mol. Cryst.,* 1968, **5**, 95–110; R. Rudman, *Mol. Cryst. Liq. Cryst.*, 1970, **6**, 427–429] the temperature of the sample was increased to 220 K and the single-crystal X-ray intensity data were collected.

A modified Merrill-Bassett diamond-anvil cell, DAC [L. Merrill and W. A. Bassett, *Rev. Sci. Instrum.,* 1974, **45**, 290–294; W. A. Bassett, *High Press. Res.*, 2009, **29**, 163–186] was used for the high-pressure freezing of a 1:1 (v/v) mixture of 111TCE and methanol, MeOH (pure p. a., POCh, Poland). A general experimental procedure for the high-pressure crystallization method was previously reported [R. Fourme, *J. Appl. Crystallogr.,* 1968, **1**, 23–30; W. L. Vos, L. W. Finger, R. J. Hemley and H. Mao, *Phys. Rev. Lett.,* 1993, **71**, 3150–3153; D. R. Allan, S. J. Clark, M. J. P. Brugmans, G. J. Ackland and W. L. Vos, *Phys. Rev. B, Condens. Mat.,* 1998, **58**, R11809–R11812; M. Bujak, A. Budzianowski and A. Katrusiak, *Z. Kristallogr.*, 2004, **63**, 573–579]. The diameter of the diamond culets was 0.8 mm. The gasket was made of 0.3 mm thick steel foil, with a 0.49 mm in diameter hole, spark-eroded and pre-indented to *ca.* 0.43 mm [A. Katrusiak, *J. Appl. Crystallogr.,* 1999, **32**, 1021–1023]. After nucleation the pressure in the DAC was slowly released until all but one crystal melted. This seed was allowed to grow, slowly increasing pressure, leading to a single crystal in the shape of prism (Fig. 2). The first

data set was collected at 0.75(5) GPa. Then the data for the same 111TCE single crystals at 1.15(5) and 2.15(5) GPa were recorded in analogous way. The ruby-fluorescence method, using a BETSA PRL spectrometer, was utilized to measure the pressure in the DAC [J. D. Barnett, S. Block and G. J. Piermarini, *Rev. Sci. Instrum.,* 1973, **44**, 1–9; G. J. Piermarini, S. Block, J. D. Barnett and R. A. Forman, *J. Appl. Phys.,* 1975, **46**, 2774–2780] with the accuracy of *ca.* 0.05 GPa.

Data collection, data reduction, structure solution and refinement

The low-temperature/ambient-pressure (0.1 MPa) and room-temperature (295 K)/high-pressure diffraction data were collected on an Oxford Diffraction diffractometers with the graphite-monochromated MoKα radiation: Xcalibur E (equipped with an Enhance X-ray source and an EOS CCD detector) and KUMA KM4-CCD, respectively. At 220.0(1) K the reflections were measured using the ω-scan technique with $\Delta\omega$ = 1.0º, and 2.14 s exposure time.

The pressure-frozen single crystals of 111TCE were centred on the diffractometer using the shadow method [A. Budzianowski and A. Katrusiak, in *High-Pressure Crystallography,* ed. A. Katrusiak and P. F. McMillan, Dordrecht: Kluwer Academic Publishers, 2004, pp. 101–112]. The room temperature/high pressure intensity data, at 0.75(5), 1.15(5) and 2.15(5) GPa, were collected using the φ- and ω-scan techniques with $\Delta\omega/\Delta\varphi$ = 1.0º and 35 s exposure time. All data were accounted for the Lorentz, polarization and sample absorption effects [Oxford Diffraction, 2009, Oxford Diffraction Ltd., *CrysAlis CCD, Data collection GUI for CCD and CrysAlis RED CCD data reduction GUI, versions 1.171.33.36d*; Oxford Diffraction, 2009, Oxford Diffraction Ltd., *CrysAlis Pro, Data collection and data reduction GUI for Pro, version 1.171.33.48*] and the high-pressure data additionally for the absorption of X-rays by the DAC and shadowing of the single crystal by the gasket edges [A. Katrusiak, REDSHABS, 2003, *Program for correcting reflections intensities for DAC absorption, gasket shadowing and sample crystal absorption.* Adam Mickiewicz University, Poznań, Poland; A. Katrusiak, *Z. Kristallogr.*, 2004, **219**, 461–467]. The structures were solved by the Patterson method and refined with SHELX-97 [G. M. Sheldrick, *Acta Cryst.* 2008, **A64**, 112–122]. The Cl and C atoms were refined with anisotropic displacement parameters. All hydrogen atoms, in the low-temperature structure, were located in subsequent maps, refined and geometrically restrained to the same distance (DFIX command of SHELXL-97). The positions of H-atoms, in the high-pressure structures, were taken from the low-temperature model and refined using geometrical restrains similar to the low-temperature structure refinement. The H-atoms displacement parameters, in all structures, were taken with coefficients 1.5 times larger than the respective parameters of the C atoms. The numbering scheme used in all reported, in this paper, structures is the same as in the ambient-pressure structures determined at 128 and 213 K [L. Silver

and R. Rudman, *J. Chem. Phys.*, 1972, **57**, 210–216], but the coordinates were moved by the [1/2 0 1] vector.

Table S1. The 111TCE crystal data and structure determination summary.

temperature, K	220.0(1)	295(2)	295(2)	295(2)
pressure	0.1 MPa	0.75(5) GPa	1.15(5) GPa	2.15(5) GPa
formula	$C_2H_3Cl_3$	$C_2H_3Cl_3$	$C_2H_3Cl_3$	$C_2H_3Cl_3$
fw, g/mol	133.39	133.39	133.39	133.39
crystal size, mm^3	0.30 x 0.30 x 0.10	0.36 x 0.20 x 0.22	0.35 x 0.23 x 0.22	0.35 x 0.24 x 0.22
crystal system	orthorhombic	orthorhombic	orthorhombic	orthorhombic
space group, Z	*Pnma*, 4	*Pnma*, 4	*Pnma*, 4	*Pnma*, 4
a, Å	11.5520(10)	11.266(2)	11.0912(19)	10.914(2)
b, Å	8.0069(7)	7.748(8)	7.588(7)	7.414(6)
c, Å	5.8733(4)	5.7183(12)	5.6253(10)	5.5350(10)
V, $Å^3$	543.26(8)	499.1(5)	473.4(5)	447.9(4)
ρ, g/cm^3	1.631	1.775	1.872	1.978
μ, mm^{-1}	1.516	1.650	1.740	1.839
θ range, °	3.53 – 25.03	3.62 – 25.05	4.06 – 25.09	4.13 – 25.09
index ranges	$-4 \le h \le 13$	$-12 \le h \le 12$	$-12 \le h \le 12$	$-12 \le h \le 12$
	$-9 \le k \le 4$	$-4 \le k \le 4$	$-4 \le k \le 4$	$-4 \le k \le 4$
	$-4 \le l \le 7$	$-6 \le l \le 6$	$-6 \le l \le 6$	$-6 \le l \le 6$
reflns collected	1302	2106	2077	1996
R_{int}	0.0184	0.1432	0.1022	0.0993
data [$I > 2\sigma(I)$]	393	203	198	193
data/parameters	515/33	213/34	208/34	199/34
GOF on F^2	0.999	1.256	1.223	1.136
R_1 [$I > 2\sigma(I)$]	0.0329	0.0586	0.0475	0.0576
R_1 (all data)[a]	0.0432	0.0628	0.0516	0.0595
wR_2 (all data)[a]	0.0866	0.1141	0.1386	0.1248
lrgst diff peak, $e/Å^3$	0.313	0.242	0.378	0.375
lrgst diff hole, $e/Å^3$	–0.250	–0.306	–0.317	–0.381

[a] $R_1 = \Sigma||F_o|-|F_c||/\Sigma|F_o|$; $wR_2 = \{\Sigma[w(F_o^2-F_c^2)^2]/\Sigma[w(F_o^2)^2]\}^{1/2}$; $w = 1/[\sigma^2(F_o^2)+(aP)^2 + bP]$, where $P = (F_o^2 + 2F_c^2)/3$

The CrysAlis CCD, CrysAlis RED and CrysAlis Pro programs [Oxford Diffraction, 2009, Oxford Diffraction Ltd., *CrysAlis CCD, Data collection GUI for CCD and CrysAlis RED CCD data reduction GUI, versions 1.171.33.36d*; Oxford Diffraction, 2009, Oxford Diffraction Ltd., *CrysAlis Pro, Data collection and data reduction GUI for Pro, version 1.171.33.48*] were used for the data collection, unit-cell refinement and data reductions (initial reduction of the high-pressure intensity data). The 111TCE crystal data and structure determination summary are listed in Table S1. The bond lengths, angles and the shortest intermolecular distances are presented in Tables S2 and S3.

The compressed intermolecular contacts have been compared using the Hirshfeld-surface analyses, provided by Crystal Explorer [S. K. Wolff, D. J. Grimwood, J. J. McKinnon, D. Jayatilaka and N. A. Spackman, 2007, *CrystalExplorer 2.0* (r 313). University of Western Australia, Perth, Australia; http://hirshfeldsurface.net/CrystalExplorer/; J. J. McKinnon, M. A. Spackman and A. S. Mitchell, *Acta Cryst.,* 2004, **B60**, 627–668].

Program *GAUSSIAN03* [M. J. Frisch, G. W. Trucks, H. B. Schlegel, G. E. Scuseria, M. A. Robb, J. R. Cheeseman, J. A. Montgomery, T. Vreven, K. N. Kudin, J. C. Burant, J. M. Millam, S. S. Iyengar, J. Tomasi, V. Barone, B. Mennucci, M. Cossi, G. Scalmani, N. Rega, G. A. Petersson, H. Nakatsuji, M. Hada, M. Ehara, K. Toyota, R. Fukuda, J. Hasegawa, M. Ishida, T. Nakajima, Y.

Honda, O. Kitao, H. Nakai, M. Klene, X. Li, J. E. Knox, H. P. Hratchian, J. B. Cross, C. Adamo, J. Jaramillo, R. Gomperts, R. E. Stratmann, O. Yazyev, A. J. Austin, R. Cammi, C. Pomelli, J. W. Ochterski, P. Y. Ayala, K. Morokuma, G. A. Voth, P. Salvador, J. J. Dannenberg, V. G. Zakrzewski, S. Dapprich, A. D. Daniels, M. C. Strain, O. Farkas, D. K. Malick, A. D. Rabuck, K. Raghavachari, J. B. Foresman, J. V. Ortiz, Q. Cui, A. G. Baboul, S. Clifford, J. Cioslowski, B. B. Stefanov, G. Liu, A. Liashenko, P. Piskorz, I. Komaromi, R. L. Martin, D. J. Fox, T. Keith, M. A. Al-Laham, C. Y. Peng, A. Nanayakkara, M. Challacombe, P. M. W. Gill, B. Johnson, W. Chen, M. W. Wong, C. Gonzalez and J. A. Pople, *GAUSSIAN*03, Revision B.04, Gaussian, Inc., Pittsburgh PA, 2003] and a PC were used at the B3LYP/3-21G** level of theory for DFT calculations of the electrostatic potential on the molecular surface of 111TCE. Electrostatic potential was mapped onto the molecular surface defined as 0.001 a.u. electron-density envelope.

Compressibility measurement

The room-temperature compressibility measurement, between ambient pressure and 1 GPa, was performed in the piston-and-cylinder apparatus [B. Baranowski and A. Moroz, *Polish J. Chem.,* 1982, **56**, 379–391]. The pressure was increased in *ca.* 20 MPa steps (Fig. 1).

Table S2. The molecular dimensions (Å, º) for 111TCE.

Atoms; Pressure/Temperature (K)	0.1 MPa/220	0.75 GPa/295	1.15 GPa/295	2.15 GPa/295
C1–Cl1	1.772(2)	1.768(6)	1.781(6)	1.769(5)
C1–Cl2	1.773(3)	1.779(8)	1.775(8)	1.778(7)
C1–C2	1.492(5)	1.524(13)	1.521(12)	1.517(11)
C2–H1	0.96(2)	0.96(2)	0.96(2)	0.96(2)
C2–H2	0.96(1)	0.96(2)	0.96(1)	0.96(1)
C2–C1–Cl1	111.22(16)	111.1(4)	110.9(4)	110.7(4)
C2–C1–Cl2	111.1(3)	109.8(7)	110.9(6)	109.9(6)
Cl1–C1–Cl1^{I}	107.75(18)	109.1(5)	108.4(5)	109.0(4)
Cl1–C1–Cl2	107.69(14)	107.8(3)	107.8(3)	108.2(3)
C1–C2–H1	110(3)	108(6)	107(5)	105(5)
C1–C2–H2	108(2)	108(5)	108(3)	111(3)
H1–C2–H2	110(2)	109(5)	111(2)	110(2)
Cl1–C1–C2–H1	–60.1(2)	–60.8(4)	–60.3(4)	–60.5(3)
Cl1–C1–C2–H2	60(2)	56(5)	60(2)	58(2)
Cl1–C1–C2–H2^{I}	180(2)	–178(5)	180(2)	–179(2)
Cl1^{I}–C1–C2–H1	60.1(2)	60.8(4)	60.3(4)	60.5(3)
Cl1^{I}–C1–C2–H2	–180(2)	178(5)	–180(2)	179(2)
Cl1^{I}–C1–C2–H2^{I}	–60(2)	–56(5)	–60(2)	–58(2)
Cl2–C1–C2–H1	180	180	180	180
Cl2–C1–C2–H2	–60(2)	–63(5)	–60(2)	–61(2)
Cl2–C1–C2–H2^{I}	60(2)	63(5)	60(2)	61(2)

Symmetry codes: (I) x, 1/2 – y, z

Table S3. The geometries (Å, º) of the shortest intermolecular interactions for 111TCE at 2.15 GPa/295 K and 1.15 GPa/295 K.

Atoms; Pressure/Temperature	2.15 GPa/295 K	Atoms; Pressure/Temperature	1.15 GPa/295 K
Cl1···Cl2^{II}	3.422(3)	Cl1···Cl2^{II}	3.509(3)
C1–Cl1···Cl2^{II}	88.3(2)	C1–Cl1···Cl2^{II}	88.9(3)
Cl1···Cl2^{II}–C1^{II}	154.83(7)	Cl1···Cl2^{II}–C1^{II}	155.25(8)
C1–Cl1···Cl2^{II}–C1^{II}	–143.0(9)	C1–Cl1···Cl2^{II}–C1^{II}	–140.4(9)
Cl1···Cl2^{III}	3.427(3)	Cl1···Cl2^{III}	3.504(4)
C1–Cl1···Cl2^{III}	152.5(3)	C1–Cl1···Cl2^{III}	153.9(3)
Cl1···Cl2^{III}–C1^{III}	103.5(2)	Cl1···Cl2^{III}–C1^{III}	104.6(2)
C1–Cl1···Cl2^{III}–C1^{III}	–126.7(4)	C1–Cl1···Cl2^{III}–C1^{III}	–126.6(5)
Cl1···H2^{IV}	2.90(5)	Cl1···H2^{IV}	3.00(5)
C1–Cl1···H2^{IV}	104.6(5)	C1–Cl1···H2^{IV}	105.3(5)
Cl1···H2^{IV}–C2^{IV}	124(4)	Cl1···H2^{IV}–C2^{IV}	122(4)
C1–Cl1···H2^{IV}–C2^{IV}	8(3)	C1–Cl1···H2^{IV}–C2^{IV}	9(2)
Cl2···Cl1^{V}	3.427(3)	Cl2···Cl1^{V}	3.504(4)
C1–Cl2···C1^{V}	109.0(2)	C1–Cl2···C1^{V}	109.7(2)
Cl2···Cl1^{V}–C1^{V}	152.5(3)	Cl2···Cl1^{V}–C1^{V}	153.9(3)
C1–Cl2···Cl1^{V}–C1^{V}	–126.7(4)	C1–Cl2···Cl1^{V}–C1^{V}	–126.6(5)
Cl2···Cl1^{VI}	3.427(3)	Cl2···Cl1^{VI}	3.504(4)
C1–Cl2···Cl1^{VI}	103.5(2)	C1–Cl2···Cl1^{VI}	104.6(2)
Cl2···Cl1^{VI}–C1^{VI}	152.5(3)	Cl2···Cl1^{VI}–C1^{VI}	153.9(3)
C1–Cl2···Cl1^{VI}–C1^{VI}	126.7(4)	C1–Cl2···Cl1^{VI}–C1^{VI}	126.6(5)
Cl2···Cl1^{VII}	3.422(3)	Cl2···Cl1^{VII}	3.509(3)
C1–Cl2···Cl1^{VII}	154.83(7)	C1–Cl2···Cl1^{VII}	155.25(8)
Cl2···Cl1^{VII}–C1^{VII}	88.3(2)	Cl2···Cl1^{VII}–C1^{VII}	88.9(3)
C1–Cl2···Cl1^{VII}–C1^{VII}	143.0(9)	C1–Cl2···Cl1^{VII}–C1^{VII}	140.4(9)
Cl2···Cl1^{VIII}	3.422(3)	Cl2···Cl1^{VIII}	3.509(3)
C1–Cl2···Cl1^{VIII}	154.83(7)	C1–Cl2···Cl1^{VIII}	155.25(8)
Cl2···Cl1^{VIII}–C1^{VIII}	88.3(2)	Cl2···Cl1^{VIII}–C1^{VIII}	88.9(3)
C1–Cl2···Cl1^{VIII}–C1^{VIII}	–143.0(9)	C1–Cl2···Cl1^{VIII}–C1^{VIII}	–140.4(9)
Cl2···H2^{IX}	2.94(1)	Cl2···H2^{IX}	3.03(1)
C1–Cl2···H2^{IX}	91.1(8)	C1–Cl2···H2^{IX}	91.4(8)
Cl2···H2^{IX}–C2^{IX}	151(2)	Cl2···H2^{IX}–C2^{IX}	152(2)
C1–Cl2···H2^{IX}–C2^{IX}	–126(9)	C1–Cl2···H2^{IX}–C2^{IX}	–131(9)
Cl2···H2^{X}	2.94(1)	Cl2···H2^{X}	3.03(1)
C1–Cl2···H2^{X}	91.1(8)	C1–Cl2···H2^{X}	91.4(8)
Cl2···H2^{X}–C2^{X}	151(2)	Cl2···H2^{X}–C2^{X}	152(2)
C1–Cl2···H2^{X}–C2^{X}	126(9)	C1–Cl2···H2^{X}–C2^{X}	131(9)
H2···Cl2^{IX}	2.94(1)	H2···Cl2^{IX}	3.03(1)
C2–H2···Cl2^{IX}	151(2)	C2–H2···Cl2^{IX}	152(2)
H2···Cl2^{IX}–C1^{IX}	91.1(8)	H2···Cl2^{IX}–C1^{IX}	91.4(8)
C2–H2···Cl2^{IX}–C1^{IX}	126(9)	C2–H2···Cl2^{IX}–C1^{IX}	131(9)
H2···Cl1^{XI}	2.90(5)	H2···Cl1^{XI}	3.00(5)
C2–H2···Cl1^{XI}	124(4)	C2–H2···Cl1^{XI}	122(4)
H2···Cl1^{XI}–C1^{XI}	104.6(6)	H2···Cl1^{XI}–C1^{XI}	105.3(5)
C2–H2···Cl1^{XI}–C1^{XI}	–8(3)	C2–H2···Cl1^{XI}–C1^{XI}	–9(2)

Symmetry codes: (II) x, y, $-1+z$; (III) $3/2-x$, $-y$, $-1/2+z$; (IV) $1/2+x$, y, $1/2-z$; (V) $3/2-x$, $-y$, $1/2+z$; (VI) $3/2-x$, $1/2+y$, $1/2+z$; (VII) x, $1/2-y$, $1+z$; (VIII) x, y, $1+z$; (IX) $1-x$, $-y$, $1-z$; (X) $1-x$, $1/2+y$, $1-z$; (XI) $-1/2+x$, y, $1/2-z$.

Table S4. The comparison of selected structural and thermodynamic parameters for low-temperature and high-pressure structures of 111- and 112TCE.

Parameter/Compound	111TCE		112TCE	
	220 K/0.1MPa	1.15 GPa/295 K	220 K/0.1 MPa	1.20 GPa/295 K
melting point, K	242.8		236.6	
boiling point, K	347.2		387.0	
density, $g \cdot cm^{-3}$	1.631	1.872	1.702	1.916
space group	*Pnma* (ordered)		$P2_1/c$ (disordered)	$P2_1/n$ (ordered)
hard-sphere volume[a], $Å^3$	67.87	68.11	85.70[b] (90.82)	84.73
packing coefficient	0.50	0.58	0.66[b] (0.70)	0.73

[a]Calculated using VOLUME [A. Katrusiak, VOLUME, 2010, *Program for calculating the volume of molecules.* Adam Mickiewicz University, Poznań, Poland]
[b]Packing coefficient for the ordered 112TCE molecule, the one with C and H 0.85 occupancy. [M. Bujak, M. Podsiadło and A. Katrusiak, *Chem. Commun.*, 2008, 4439–4441].

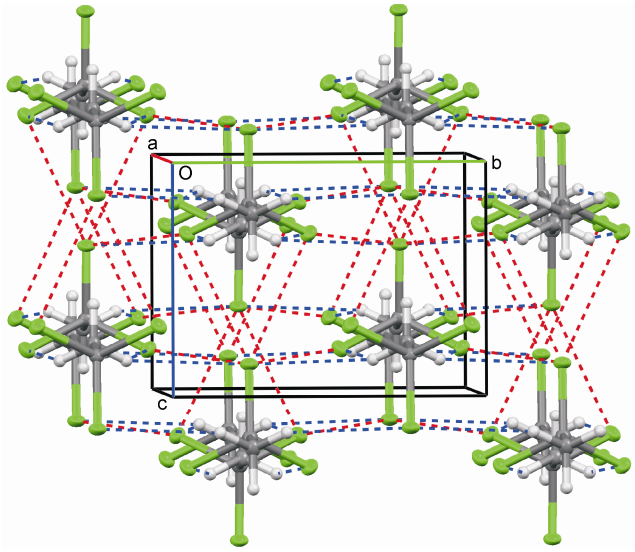

Fig. S1. The crystal structure of 111TCE at 2.15 GPa/295 K. The dashed red and blue lines indicate the shortest Cl···Cl and Cl···H intermolecular distances, respectively (Table S3). Displacement ellipsoids are plotted at the 25% probability level.

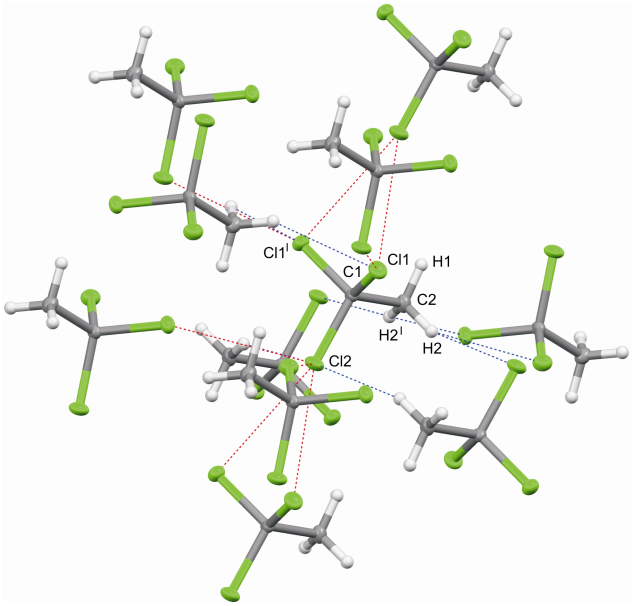

Fig. S2. The Cl···Cl and Cl···H intermolecular contacts denoted by the red and blue dashed lines, respectively, made by the single 111TCE molecule at 2.15 GPa/295 K (Table S3). Displacement ellipsoids are plotted at the 25% probability level. Symmetry code: (^{I}) x, 1/2 – y, z.

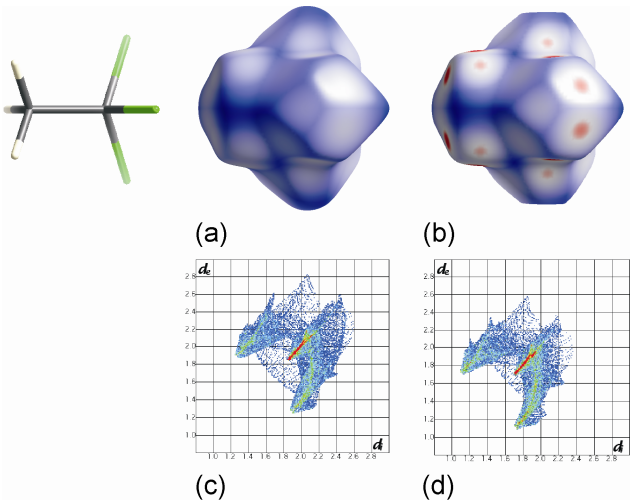

Fig. S3. The Hirshfeld surfaces for the 111TCE molecule at (*a*) 220 K/0.1 MPa and (*b*) 2.15 GPa/295 K. The color scale describes distances longer (shades of navy-blue), equal (white) and shorter (red) than van der Waals radii. Two-dimensional fingerprint plots for the structures of 111TCE at (*c*) 220 K/0.1 MPa and (*d*) at 2.15 GPa/295 K.

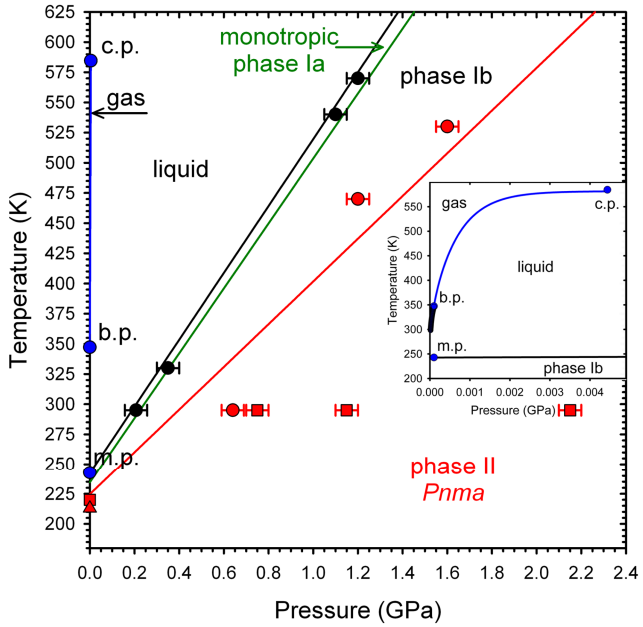

Fig. S4. The phase diagram of 111TCE; the critical point c.p. at 4.4 MPa, 584.5 K [G. Sivaramprasad, M. V. Rao and D. H. L. Prasad, *J. Chem. Eng. Data*, 1990, **35**, 122–124]), the melting (m.p. 242.8 K) and boiling points (b.p. 347.2 K) [D. R. Lide, *CRC Handbook of Chemistry and Physics*, 75th ed.; CRC Press Inc.: Boca Raton, FL, 1994] (blue circles); the transition boundaries between liquid/phase Ia, phases Ia/Ib, and phases Ib/II are indicated by the black, green and red lines, respectively after Würflinger and Pardo [A. Würflinger and L. C. Pardo, *Z. Naturforsch.,* 2002, **57a**, 177–183]; the freezing points (black circles) and Ib → II transition point both at 295 K (red circle) are from the piston-cylinder press (Fig. 1) and above 295 K from optical observation of 111TCE melting in the DAC; red circles above 295 K indicate Ib → II transition points from optical observation in the DAC (spectroscopic pressure calibration and a thermocouple temperature measurement); the structural diffractometric determinations in phase II are denoted by the red squares – this work; and a red triangle [L. Silver and R. Rudman, *J. Chem. Phys.*, 1972, **57**, 210–216]. The gas-liquid region is shown in the inset: the experimental vapor-pressure data (black points) [F. Corelli and R. Francesconi, *J. Chem. Eng. Data*, 1995, **40**, 21–24] and the gas-liquid boundary extrapolation (blue line).